Science of the Total Environment 835 (2022) 155478

Contents lists available at ScienceDirect

Science of the Total Environment

journal homepage: www.elsevier.com/locate/scitotenv

# Alongshore upwelling modulates the intensity of marine heatwaves in a temperate coastal sea

Paula Izquierdo [a,*], Fernando González Taboada [b,c], Ricardo González-Gil [d], Julio Arrontes [a], José M. Rico [a]

[a] Departamento de Biología de Organismos y Sistemas, Unidad de Ecología, Universidad de Oviedo, C/ Catedrático Rodrigo Uría s/n, 33071 Oviedo, Spain
[b] Atmospheric and Oceanic Sciences Program, Princeton University, Princeton, NJ 08540, USA
[c] AZTI Marine Research, Basque Research and Technology Alliance (BRTA), Txatxarramendi Ugartea z/g, 48395 Sukarrieta, Spain
[d] Department of Mathematics and Statistics, University of Strathclyde, UK

## HIGHLIGHTS

- We analyzed marine heatwaves based on satellite and field, near-shore temperatures.
- Satellites detect open ocean heatwaves but overestimate near-shore ones.
- Alongshore upwelling prevents open ocean marine heatwaves from reaching the shore.
- We develop a method to clear satellite biases and reconstruct near-shore heatwaves.
- Half of the six-fold increase in marine heatwaves seems related to ocean warming.
- Accounting for sea warming reduces to half the increasing trend in marine heatwaves.

## GRAPHICAL ABSTRACT

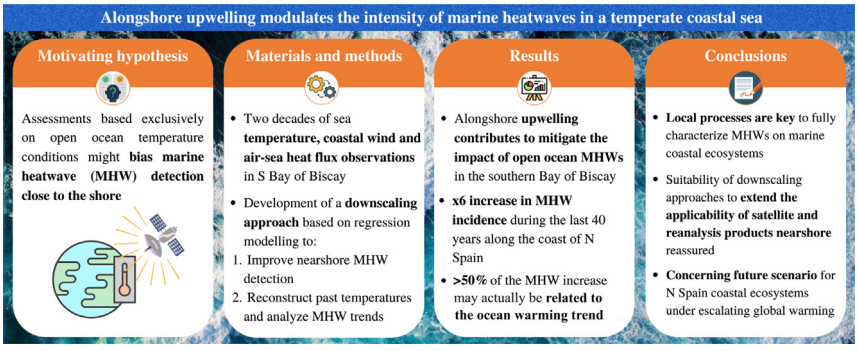


## ARTICLE INFO

Editor: Martin Drews

*Keywords:*
Sea surface temperature
Global warming
Ocean remote sensing
Climate refugia
Shelf seas
Bay of Biscay

## ABSTRACT

Analyses of long-term temperature records based on satellite data have revealed an increase in the frequency and intensity of marine heatwaves (MHWs) in the world oceans, a trend directly associated with global change according to climate model simulations. However, these analyses often target open ocean pelagic systems and rarely include local scale, field temperature records that are more adequate to assess the impact of MHWs close to the land-sea interface. Here, we compared the incidence and characteristics of open ocean MHWs detected by satellites with those observed in the field over two decades (1998–2019) at two temperate intertidal locations in the central Cantabrian Sea, southern Bay of Biscay. Satellite retrievals tended to smooth out cooling events associated with intermittent, alongshore upwelling, especially during summer. These biases propagated to the characterization of MHWs and resulted in an overestimation of their incidence and duration close to the coast. To reconcile satellite and field records, we developed a downscaling approach based on regression modeling that enabled the reconstruction of past temperatures and analyze MHW trends. Despite the cooling effect due to upwelling, the temperature reconstructions revealed a six-fold increase in the incidence of MHWs in the Cantabrian Sea over the last four decades. A comparison between static (no trend) *vs.* dynamic (featuring a linear warming trend) MHW detection thresholds allowed us to attribute over half of the increase in MHW incidence to the ocean warming trend. Our results highlight the importance of local processes to fully characterize the complexity and impacts of MHWs on marine coastal ecosystems and call for the conservation of climate refugia associated with coastal upwelling to counter the impacts of climate warming.

* Corresponding author.
*E-mail address:* uo245718@uniovi.es (P. Izquierdo).

http://dx.doi.org/10.1016/j.scitotenv.2022.155478
Received 3 February 2022; Received in revised form 14 April 2022; Accepted 19 April 2022
Available online 23 April 2022

## 1. Introduction

Marine heatwaves (MHWs) are transient episodes of extreme water temperatures that leave a detrimental and long-lasting impact on the structure and functioning of marine ecosystems (Hobday et al., 2016; Oliver et al., 2021). Analyses of long-term satellite temperature records have revealed an increase in the frequency, intensity and duration of MHWs during the last century (Oliver et al., 2018). Such trends parallel the gradual increase in ocean temperature due to anthropogenic greenhouse gas emissions (Gulev et al., 2021), which lies behind the dramatic increase in the occurrence and intensity of MHWs in recent decades (Laufkötter et al., 2020). In fact, projections under different socioeconomic development scenarios foresee a sustained increase in the likelihood and severity of MHWs around the world in coming years (Frölicher et al., 2018; Fox-Kemper et al., 2021).

Discrete events like MHWs often pose a more serious threat to marine life than changes in mean state due to the sudden and long-lasting consequences triggered by extreme perturbations (O'Leary et al., 2017). Fluctuations and extremes in water temperature are an intrinsic component of environmental variability that shapes the structure and functioning of marine ecosystems (Denny et al., 2009; Clarke, 2017). In practice, despite growing concerns, analyzing the impact of MHWs becomes a complex task. Temperature extremes leading to MHWs are by definition rare, short-lived warming episodes above normal conditions that often last for a few days. As a consequence, the detection and characterization of MHWs remains challenging and demands sustained records of high-frequency observations.

Long-term temperature records are necessary to define a meaningful baseline and characterize extremes, while high-quality, frequent observations are important to avoid biases and ensure the proper detectability of MHW events (Hobday et al., 2016; WMO, 2018). Such constraints become more acute when attempting to characterize changes in the incidence and intensity of MHWs. High data demands make that most MHW studies tend to rely on satellite or model-based datasets, and to focus on open ocean pelagic environments away from the coastline, where the presence of land and local processes like river runoff and coastal upwelling limit indirect approaches (Smit et al., 2013; Stobart et al., 2016; Schlegel, 2017). These biases may extend to the detection of small-scale variability and temperature extremes (Smale and Wernberg, 2009; Smit et al., 2013). In fact, it has been recently shown that remotely-sensed products may overestimate coastal SSTs in upwelling prone locations (Meneghesso et al., 2020) as a result of the differences between the warming rates in offshore *vs.* nearshore waters (Varela et al., 2018), which may ultimately lead to the overestimation of MHW trends (Varela et al., 2021). This raises concerns about the actual impact of MHWs in coastal areas.

Intertidal and shallow coastal areas disproportionately contribute valuable ecosystem services to humankind (Costanza et al., 2014). These highly diverse and productive habitats control land erosion and buffer coastal pollution through carbon sequestration and nutrient cycling (Barbier, 2017). They also provide commodities ranging from fertilizers and foods to compounds of industrial use, which are harvested from algae and fisheries or collected from aquaculture. MHWs compromise the sustained provision of these services and the restoration of currently degraded ecosystems (Duarte et al., 2020), and represent a threat to blue carbon nature-based solutions that may contribute to mitigate climate change (Macreadie et al., 2021). Together, these issues call for an improved monitoring and assessment of the impact of MHWs in coastal areas as a way to guide the sustainable use and conservation of living marine resources.

Here, we analyze the incidence of MHWs along the coasts of the central Cantabrian Sea, in the Northeast Atlantic. This stretch covers a sharp biogeographical transition from cool to warm conditions where temperature extremes have prompted abrupt changes in the structure of coastal marine communities in recent years (Viejo et al., 2011; Fernández, 2011; Voerman et al., 2013; Fernández, 2016). Taking advantage of high-frequency, two-decade long temperature field records, we assessed the reliability of coarse scale satellite data to monitor MHWs in coastal areas. The analyses revealed important biases that resulted in the overestimation of the incidence of MHWs by satellites during periods of intense upwelling. To reconcile satellite and field measurements we developed a statistical downscaling approach, a technique often used to obtain finer-scale climate information from coarse resolution products (see Wilby and Wigley, 1997). Such approach enabled us to account for the impact of upwelling on nearshore temperatures, exploit the prolonged coverage of the satellite record and hindcast the incidence of MHWs during the last four decades. We characterized MHWs using two different baseline periods: static -based on the climatological seasonal cycle- *vs.* dynamic-featuring a linear warming trend-. The comparison of both approaches provides useful insight on the potential contribution of climate warming to the increased incidence of MHW. Our results highlight the contribution of upwelling to buffer the impact of open ocean MHWs in coastal areas, but in parallel reveal a concerning increase in the incidence and intensity of MHWs due to climate warming.

## 2. Materials and methods

### 2.1. Study area

We analyzed the occurrence and intensity of MHWs in the central Cantabrian Sea (Fig. 1), a narrow (30–40 km) temperate coastal shelf sea located in the southern Bay of Biscay (NE Atlantic, Gil et al., 2002). To this end, we combined data from large scale ocean reanalysis and satellite monitoring of the temperature of the ocean surface with field measurements at two selected coastal locations —Oleiros (6.200°W 43.575°N) and La Franca (4.575°W 43.395°N)— which enabled us to assess and calibrate satellite data (Fig. 1).

Large scale gradients in ocean conditions anticipate spatial variability in the incidence and characteristics of MHWs along the entire Cantabrian Sea. Water temperatures increase eastwards as climatic conditions become less oceanic and more continental due to the proximity of the Eurasian landmass (Koutsikopoulos et al., 1998). Atmospheric circulation further presents a marked seasonality, with prevailing southwesterly winds during autumn and winter, and northeasterly winds during spring and summer that are more intense towards the west. The easterly component flows parallel to the coast and causes intermittent upwelling events that, especially during summer, bring cool waters to the surface and erode the seasonal thermal stratification of the upper layer (Gil et al., 2002), further contributing to accentuate the eastward gradient in temperature (Botas et al., 1990).

Oleiros and La Franca are representative of large-scale gradients in environmental conditions in the Cantabrian Sea and their effect on marine life. The two locations are separated by just ~100 km of coast but, halfway amid them, the presence of Cape Peñas alters the predominant east-west orientation of the coastline (Fig. 1). This headland juts 10 km into the sea, affecting coastal circulation by deflecting internal waves and enhancing the gradient towards more intense seasonal alongshore upwelling in the west (Lavín et al., 2006; Llope et al., 2006). As a consequence, the cape marks the approximate location of a sharp biogeographical transition from cool to warm adapted intertidal communities towards the interior of the Bay of Biscay (Anadón and Niell, 1980). Both locations are otherwise similar; they are rocky shores exposed to the open ocean, located away of any known anthropogenic heat source, and experiencing moderate semidiurnal tides with a range of up to 4.5 m during the spring tides.

### 2.2. Temperature time series and ancillary datasets

The incidence of MHWs was analyzed based both on field and remote sensing temperature time series data. To examine potential biases among the two data sources, we further retrieved time series of alongshore upwelling and of heat fluxes across the air-sea interface, which provided a proxy of water column stratification.

#### 2.2.1. Field temperature data

Daily field temperature measurements were collected at Oleiros and La Franca from Jan. 1998 to Mar. 2019 (~21 years) using TidbiT V2 water

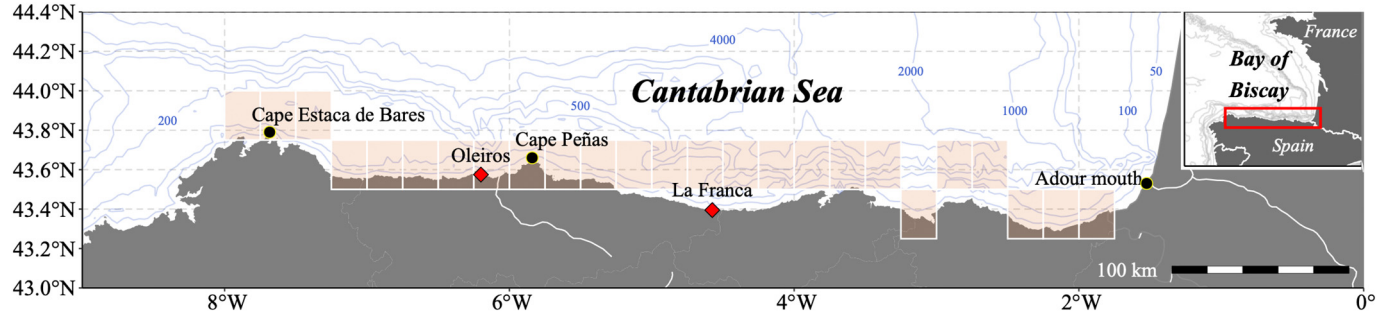


**Fig. 1.** Map of the Cantabrian Sea showing the study areas of Oleiros and La Franca, where the field observations were collected. Salmon-colored rectangles represent the 0.25° localities covering the spatial extent of the extended modelled temperature series ($n = 25$). The locations of Cape Estaca de Bares and the mouth of the Adour River serve as reference to indicate the edges of the extended series. Bathymetry data were extracted from the GEBCO 2021 Grid (GEBCO Compilation Group, 2021).

temperature dataloggers (Onset Computer Corp). The loggers were attached to the rock and protected from wave action by a steel mesh. Temperature data were retrieved with a HOBO Optic USB Base Station reader and converted to text files using HOBOWare Pro v.3.7.10 (Onset Computer Corp). These devices have a maximum sustained temperature range of 0°-30 °C in water and an accuracy of ±0.21 °C over 0°–50 °C. The dataloggers were programmed to retrieve a single datum per hour before attaching them at depths 0.3–0.6 m above the lowest astronomical tide to ensure they were always submerged at high tide. The time series was filtered to retain the two records per day that correspond to water temperature at semidiurnal high tides. Then the average of high tide values was calculated to estimate daily mean sea temperature and applied a backward 5-day moving average to smooth out high frequency noise. The resulting daily series was 21 years long but presented ~6% and ~ 18% missing data at Oleiros and La Franca, respectively. Though time series with these features would be considered sub-optimal according to Hobday et al. (2016) recommendations, they remain suitable for MHW research (Schlegel et al., 2019).

*2.2.2. Satellite temperature data*

Sea surface temperature (SST) data were retrieved for the entire coast of the Cantabrian Sea from the NOAA Optimum interpolation 0.25° daily sea surface temperature analysis (oiSST version 2, Sep. 1981–2019, see Reynolds et al., 2007, Banzon et al., 2016 and www.ncdc.noaa.gov/oisst for further details). The assessment with field observations used data for the nearest pixel locations to the study sites (6.125°W 43.625°N for Oleiros; 4.625°W 43.625°N for La Franca). To ensure temporal homogeneity (Reynolds and Chelton, 2010), we used the Advanced Very High-Resolution Radiometer (AVHRR-only) product from the Pathfinder Version 5 dataset (Casey et al., 2010). This dataset includes an optimal interpolation step to fill gaps and aggregate fine scale high resolution retrievals (~1 km) that effectively smooths original observations and avoids biases in measurements close to the land-sea interface. Therefore, satellite-based SSTs provide a reliable temperature record for monitoring MHW incidence in open ocean waters (Hobday et al., 2016).

*2.2.3. Coastal winds and upwelling*

Hourly wind speed vectors over the ocean surface were extracted from ERA5 0.25° reanalysis data from the nearest pixel locations to the study sites (6.25°W 43.75°N for Oleiros; 4.5°W 43.5°N for La Franca), for the period Jan. 1981–Dec. 2019. Data were retrieved from the Copernicus Climate Change Service (C3S) of the Climate Data Store (CDS) (Hersbach et al., 2020). Wind stress, $\tau$ [N m$^{-2}$], was calculated from neutral wind speed vectors at 10 m ($U_{10}$ [m s$^{-1}$]) using the bulk formula; $\tau = \rho_{air} \cdot C_D \cdot U_{10} \cdot |U_{10}|$, where $\rho_{air}$ is air density (taken as 1.223 kg m$^{-3}$) and $C_D$ is a non-dimensional drag coefficient. $C_D$ was estimated as a function of $U_{10}$ based on Large et al. (1994):

$$10^3 C_D = \frac{2.70}{U_{10}} + 0.142 + 0.0764 U_{10}$$

Alongshore coastal upwelling was then calculated based on estimates of the seaward Ekman transport ($T$ [m$^2$ s$^{-1}$]) along a segment of coast of a given length ($L = 1$ m), which gives Bakun (1973) upwelling index, $bui = TL = \frac{\tau_a L}{\rho_{sw} f}$ [m$^3$ s$^{-1}$]. Transport depends on the alongshore component of wind stress, $\tau_a$, which was estimated assuming a prevailing east-west orientation of the coastline; seawater density, $\rho_{sw}$, set to 1025 kg m$^{-3}$, and the Coriolis parameter $f = 9.96\ 10^{-5}$ s$^{-1}$, corresponding to 43°N. An 11-day simple moving average was applied on the resulting *bui* estimates to integrate the cumulated impact of high frequency wind variability on cross-shore transport (Otero and Ruiz-Villarreal, 2008; García-Reyes and Largier, 2010). Positive *bui* values correspond to the upwelling of deep waters and leads to surface cooling, whereas negative values correspond to downwelling, sinking and warming.

*2.2.4. Air-sea heat fluxes and stratification*

Time series of ocean surface net heat flux, $Q_i$ [W m$^{-2}$], were calculated based on data from the Modern-Era Retrospective analysis for Research and Applications version 2 (MERRA-2) V5.12.4 ocean surface diagnostics product (M2T1NXOCN, Global Modeling & Assimilation Office [GMAO], 2015). Hourly estimates were retrieved for each 0.5° × 0.625° grid cell corresponding to the nearest pixel locations to the study sites (6.2500°W 43.75°N for Oleiros; 4.6875°W 43.5°N for La Franca), for the period Jan. 1980–Oct. 2020.

Surface waters in the Cantabrian Sea follow the characteristic seasonal cycle of temperate shelf seas (*e.g.*, Simpson and Sharples, 2012). During winter (Dec-Feb), convective mixing leads to the formation of a deep homogeneous layer that lasts until spring (Mar-May), when favorable weather conditions eventually generate a shallow, mixed layer that persists throughout summer (Jun-Aug) until autumn (Sep-Nov) storms break stratification (Lavín et al., 2006). Surface heat exchange is the dominant buoyancy source for seasonal mixing in most shelf seas, so the net heat flux ($Q_i$) was used as a proxy for thermally driven seasonal stratification (with positive [negative] $Q_i$ matching seasonal stratification [mixing]). Net heat flux was calculated as $Q_i = Q_s(1\text{-}A) - Q_b - Q_e - Q_c$, where $Q_s$ represents solar inputs to the ocean surface, $A$ is albedo, $Q_b$ *is* back radiation, $Q_e$ and $Q_c$ are sensible and latent heat fluxes respectively. An 81-day simple moving average was applied to smooth out a signal to distinguish seasonal stratification *vs.* mixing periods.

*2.3. Detectability and trends in coastal marine heatwaves (MHWs)*

The analysis was structured in three steps. First, a set of regression models was developed to downscale and calibrate the satellite time series against field observations, which allowed us to explore potential biases among the two series due to the proximity to land. Then, the impact of deviations among satellite and local field measurements on the detection and characterization of MHWs was examined. In a third set of analyses, the models were used to reconstruct past temperatures and assess the

contribution of the underlying warming trend on the incidence of MHWs in the Cantabrian Sea.

#### 2.3.1. Assessment and downscaling of satellite temperatures

In the first analysis, we tested a set of nested statistical downscaling models to assess and reconcile potential deviations between satellite temperatures and those recorded in the field (Table 1). Downscaling is a technique that allows to derive finer-scale projections of climate variables affected by local processes not captured by coarse resolution products (see Wilby and Wigley, 1997). All models initially assumed that field temperatures are linearly related to satellite retrievals. Such relationship accounts for the expected offset between field point measurements and the large areas averaged by the satellite. Local site effects account for extra deviations due to the unique characteristics of each location, from local bathymetry and circulation to the degree of land contamination in satellite retrievals.

The baseline model featured the above defined assumption of a simple linear relationship between field and satellite temperature measurements with a different intercept on each site ($T_f = \beta_0 + \beta_1 site + \beta_2 T_s$, $Mod_1$ in Table 1). Deviations between both series may grow during coastal upwelling and downwelling depending on water column stratification, so we tested two extra models, $Mod_2$ and $Mod_3$, which feature an interaction between *bui* as a proxy of cross-shore transport and net heat flux ($Q_i$) as a proxy of stratification. The interaction term accounts for the varying impact of upwelling on surface temperature; coastal upwelling (downwelling) may cool (further warm) surface waters when the column is stratified. However, upwelling may not alter surface temperatures when the column is fully mixed in winter, though downwelling may still transport slightly warmer waters from deeper areas offshore.

$Mod_2$ and $Mod_3$ attempt to capture potential differences in surface water temperatures near the shore *vs.* more oceanic conditions. $Mod_2$ is a linear regression model where the interaction between cross-shore transport and net heat flux is assumed to be linear (*i.e.*, a multiplicative, symmetric effect see $Mod_2$ in Table 1). On the other hand, $Mod_3$ is a generalized additive model (GAMs; Hastie and Tibshirani, 1986; Wood, 2017), a type of model especially useful to describe non-linear effects of independent variables without an *a priori* specification of the functional relationships (see $Mod_3$ in Table 1). In particular, $Mod_3$ includes regular smooth terms (s, specifically a thin-plate regression spline) to describe individual non-linear effects of *bui* and $Q_i$, and a tensor product smooth (*ti*) to incorporate their interactive non-linear effect and account for their different units (Wood, 2017). Such interaction enables a varying effect of cross-shore transport on deviations between satellite and field temperatures across net heat flux levels. The complexity of smooth terms in GAMs is determined through cross-validation to avoid overfitting (Wood, 2017).

$Mod_3$ assumes that the effect of upwelling on satellite deviations is homogeneous along the coast. To assess the reliability of this assumption, we reconstructed the field signal at La Franca using satellite, *bui* and *Qi* data from the closest pixel and the parameters derived from fitting of $Mod_3$ only using data from Oleiros, and vice versa. As shown in Figs. S1 and S2 in the Supplement, these analyses result in predictions i) that reproduce near-shore SSTs more reliably than the satellite (Fig. S1) and ii) comparable to those based on a model trained using all data and featuring a local upwelling effect (Fig. S2), suggesting that $Mod_3$ may provide a reasonable description of the effect of upwelling along the coast.

Model fits were checked for $Mod_1$, $Mod_2$ and $Mod_3$ for the presence of any non-random pattern in the residuals, and then ranked them using the Akaike's Information Criterion (AIC, Burnham and Anderson, 2002).

#### 2.3.2. Detection and characterization of marine heatwaves (MHW)

We analyzed the incidence and magnitude of MHWs following Hobday et al. (2016) criteria, who defined MHWs as warm periods that last for five or more consecutive days during which temperature rises above a seasonal climatology of the 90th percentile ($P_{90}$) of the temperature at a given location. Previous studies estimated $P_{90}$ threshold climatologies using a centered 30-day moving window. Such an approach introduces a directional lag by pooling temperatures consistently increasing or decreasing along the seasonal cycle. For instance, $P_{90}$ estimates for late July are partially based on warmer temperatures from early August, making it more difficult to detect actual MHWs. To avoid potential biases, we implemented a parametric Monte Carlo approach to estimate $P_{90}$. For each SST time series, we fitted a GAM featuring a constant seasonal cycle and a linear trend. Then, we randomly sampled 10,000 model parameter vectors from their fitted mean and covariance using a multivariate normal random number generator. Sample parameters were used to simulate daily surrogate time series, providing a large sample to retrieve unbiased estimates of $P_{90}$ for each simulated date. Surrogates incorporating only the constant seasonal cycle term result in a static threshold that does not vary between years, but adding simulated trends result in a time-moving $P_{90}$ threshold. This dynamic threshold is useful to assess the impact of long-term trends in MHWs (see Section 2.3.5 below). Resulting thresholds were further smoothed using a 15-day central moving average to avoid wiggles.

#### 2.3.3. Assessment of MHWs based on field observations

The second analysis focused on the incidence of MHWs at the two study locations of Oleiros and La Franca. The incidence and characteristics of MHWs were compared based on field, satellite and model-based reconstructions of coastal sea surface temperature during the period Jan. 1998–Mar. 2019. MHW detection thresholds were calculated using all available data to characterize overall changes in the incidence of MHWs. We constructed presence-absence confusion matrices to assess the ability of each temperature series to detect MHWs, setting field observations as reference (Allouche et al., 2006). Additionally, we analyzed other MHW features such as duration (*dur*) and maximum, mean and accumulated intensity of detected events ($i_{max}$, $i_{mean}$, $i_{cum}$, respectively; Hobday et al., 2016). To ensure a fair comparison, missing dates in temperature field records were masked on both satellite and model-based temperature reconstructions before the analysis and separately at each station.

#### 2.3.4. Temperature reconstruction and association of MHWs to climate warming

In the third analysis we used the best fitting model ($Mod_3$ in Table 1, based on AIC scores) to hindcast coastal temperature variability based on

**Table 1**
Model selection table summarizing the assessment of alternative hypotheses about the best strategy to reconcile satellite and field temperature measurements. Models with a lower AIC score were favored. $T_f$ stands for field measurements [°C]. Predictor variables are *site* (study area), $T_s$ (satellite measurements [°C]), *bui* (Bakun Upwelling Index [$10^3$ $m^3$ $s^{-1}$ $km^{-1}$]) and *Qi* (net heat flux [W $m^{-2}$]). The coefficient $\beta_0$ denotes the intercept, whereas the other β measure the effect of each predictor separately. $Mod_1$ and $Mod_2$ are linear models, $Mod_3$ is a Generalized Additive Model (GAM). In $Mod_3$, *s(x)* stands for a regular smooth term (specifically a thin-plate regression spline) featuring a flexible relationship between $T_f$ and the covariate *x*, while *ti*(*x*,*y*) represents a tensor smooth allowing a nonlinear interaction between covariates *x* and *y*, which may have different measurement units (Wood, 2017).

| Name | Description | Equation | logLik | dLogLik | df | AIC | dAIC | AIC weights |
|---|---|---|---|---|---|---|---|---|
| $Mod_1$ | Linear effect of satellite temperature series ($T_s$) and different intercept depending on *site*. | $T_f = \beta_0 + \beta_1 site + \beta_2 T_s$ | −18.03 | 0 | 4 | 36.07 | 7304 | 0 |
| $Mod_2$ | $T_s$ linear effect and linear interactive effect between coastal up/downwelling (*bui*) and net heat flux at the sea surface ($Q_i$). | $T_f = \beta_0 + \beta_1 site + \beta_2 T_s + \beta_3 bui + \beta_4 Q_i * Q_i$ | −15.56 | 2465 | 7 | 31.14 | 2380 | 0 |
| $Mod_3$ | $T_s$ linear effect and non-linear interactive effect between *bui* and $Q_i$ at the sea surface. | $T_f = \beta_0 + \beta_1 site + \beta_2 T_s + s_1(bui) + s_2(Q_1) + ti(bui, Q_i)$ | −14.35 | 3676 | 27 | 28.76 | 0 | 1 |

satellite and ocean reanalysis data. This approach enabled us to extend the analysis back in time and to examine trends in the incidence of MHWs during the last four decades (Sep. 1981–Dec. 2019). Also, the spatial extent was broadened to cover the entire Cantabrian Sea from Cape Estaca de Bares in the west to the mouth of the Adour River in the east ($n = 25$, Fig. 1). Upwelling index (*bui*) and heat flux ($Q_i$) reanalysis fields were aligned with SST data using first-order, conservative interpolation.

Finally, we assessed changes in trend estimates for the incidence and features of MHWs resulting when using a static detection threshold based on the climatological seasonal cycle *vs.* a dynamic baseline incorporating a linear warming trend (Oliver et al., 2021). For $i_{max}$, $i_{mean}$, $i_{cum}$ and *dur* of detected MHWs, these trends were estimated using simple linear regression (*e.g.*, Chandler and Scott, 2011). MHW frequency and the number of MHW days per year are discrete variables (*i.e.*, counts of events during some period of time) whose residuals are usually skewed following a Poisson distribution, so these trends were estimated using Poisson generalized linear models (*e.g.*, Gelman and Hill, 2007). We performed standard residual checks and tests to assess model adequacy and accounted for overdispersion of MHW counts when necessary (Gelman and Hill, 2007).

#### 2.3.5. Technical implementation details

Statistical model fitting was implemented in *R* version 4.1.2 (R Core Team, 2021) making extensive use of libraries *mgcv* (Wood, 2017) for GAMs, *caret* (Kuhn, 2020) and *bbmle* (Bolker, 2020) for confusion matrices and model predictions. MHW events were detected and characterized using the library *heatwaveR* (Schlegel and Smit, 2018), which implements the definition of MHW proposed by Hobday et al. (2016). Libraries *tidyverse* (Wickham et al., 2019), *ncdf4* (Pierce, 2019), *lubridate* (Grolemund and Wickham, 2011), *plyr* (Wickham, 2011), *zoo* (Zeileis and Grothendieck, 2005), *gratia* (Simpson, 2021), *reshape2* (Wickham, 2007), *fields* (Nychka et al., 2017), *data.table* (Dowle and Srinivasan, 2021), *sf* (Pebesma, 2018), *RColorBrewer* (Neuwirth, 2014), *cowplot* (Wilke, 2020), *rnaturalearth* (South, 2017) and *extrafont* (Chang, 2014) were also used in the analyses and to prepare graphs and other summaries.

## 3. Results

Satellite and field records of the ocean surface confirmed the predominance of cooler conditions in the westernmost station of Oleiros than in La Franca (Table 2). Differences in surface water temperatures between the two stations further increased during spring and summer coinciding with the upwelling season (Apr-Sep; Lavín et al., 2006), which is also stronger at Oleiros. The analysis also revealed large deviations between field and satellite temperature records (RMSE >1.22 °C at both Oleiros and La Franca), which increased again during the upwelling season, when satellite temperatures tended to overestimate field temperatures by up to 5 °C (Table 2, Fig. 2, Fig. S3 & Fig. S4 in Supplementary File). Satellite retrievals also resulted in smoother time series that lacked sudden temperature fluctuations associated with upwelling and downwelling events in field series.

### 3.1. Assessment and downscaling of satellite temperatures

Table 1 summarizes the assessment of models reconciling field and satellite temperature time series. Model selection based on AIC scores favored model $Mod_3$, which features a nonlinear interaction between upwelling and time-integrated heat. In essence, $Mod_3$ lowers and raises satellite temperatures during upwelling and downwelling events when $Q_i > 0$, respectively (Fig. 3). The same model further suggests that satellite temperatures tend to overestimate coastal field measurements in the absence of water column stratification ($Q_i < 0$ in Fig. 3). The model resulted nonetheless in an excellent skill ($r = 0.97$; $r2 = 0.94$), so we proceeded to reconstruct a gap-free temperature time series at the two study locations for the period Jan. 1998–Mar. 2019 (Fig. 2, Fig. S3 & Fig. S4). As expected, the reconstructed time series amended biases between field and satellite records due to wind-driven, cross-shore transport, especially during spring and summer (RMSE <0.67 °C between field and reconstructed temperatures at both Oleiros and La Franca; see Table 2 for complementary metrics).

### 3.2. Detection of MHWs in field, satellite and model-based reconstructions

Deviations between temperature time series propagated to the detection of MHW, and both the number and characteristics of the MHWs showed consistent differences between the two locations in the field, satellite and reconstructed temperature time series. The overall number of MHWs detected in the field series was 42 and 30 at Oleiros and La Franca, respectively, suggesting regional scale asynchrony in the occurrence of MHWs. The number of MHWs detected was similar and slightly larger both in the satellite and modelled series than in the field, with smaller differences with respect to MHW counts in Oleiros (41 and 46, respectively) than in La Franca (35 and 36, respectively). The satellite and the reconstructed series also failed to detect a large proportion of MHW days (above a half in Oleiros, Table 3). However, the modelled series improved the detection of MHW with respect to the raw satellite series, both in terms of MHW and non-MHW days (Table 3). The satellite series resulted in an overestimation of the incidence of MHWs, with a large proportion of false positive MHW days during upwelling episodes (*i.e.*, ~73% and ~76% of the non-MHW days classified as MHW days at Oleiros and La Franca, respectively). The same fraction is reduced at least by a half in the model-based, reconstructed series (17% and 37% of false positives during upwelling events).

### 3.3. Trends in MHWs based on temperature reconstructions

The extended series reconstructed from satellite and reanalysis data (Sep. 1981–Dec. 2019) revealed an average rate of warming of 0.16 °C per decade along the coasts of the Cantabrian Sea (Table S1 in Supplementary File). Such rate exceeds mean surface warming in the global ocean (0.11–0.13 °C per decade, Rhein et al., 2013), but it is still considerably below the estimate based on the satellite series (0.23 °C per decade,

**Table 2**
Annual and seasonal estimates of mean sea surface temperature and of the Bakun upwelling index values at Oleiros and La Franca for the period 1998–2019.

| | | | Oleiros | | | La Franca | | |
|---|---|---|---|---|---|---|---|---|
| | | | Field | Satellite | Model | Field | Satellite | Model |
| Annual | Sea surface temperature [°C] | Mean | 15.13 | 15.73 | 15.19 | 15.48 | 16.14 | 15.47 |
| | | SD | 1.14 | 1.24 | 1.10 | 1.23 | 1.32 | 1.23 |
| | Bakun Upwelling Index [$10^3 m^3 s^{-1} km^{-1}$] | Mean | – | −0.10 | – | – | −0.20 | – |
| | | SD | – | 0.77 | – | – | 0.88 | – |
| Spring-summer (Mar-Aug) | Sea surface temperature [°C] | Mean | 15.61 | 16.11 | 15.50 | 15.89 | 16.53 | 15.92 |
| | | SD | 1.23 | 1.27 | 1.19 | 1.31 | 1.40 | 1.23 |
| | Bakun Upwelling Index [$10^3 m^3 s^{-1} km^{-1}$] | Mean | – | −0.01 | – | – | −0.11 | – |
| | | SD | – | 0.65 | – | – | 0.73 | – |
| Autumn-winter (Sep-Feb) | Sea surface temperature [°C] | Mean | 14.65 | 15.35 | 14.73 | 15.09 | 15.77 | 15.03 |
| | | SD | 1.04 | 1.20 | 1.01 | 1.15 | 1.25 | 1.04 |
| | Bakun Upwelling Index [$10^3 m^3 s^{-1} km^{-1}$] | Mean | – | −0.20 | – | – | −0.29 | – |
| | | SD | – | 0.89 | – | – | 1.04 | – |

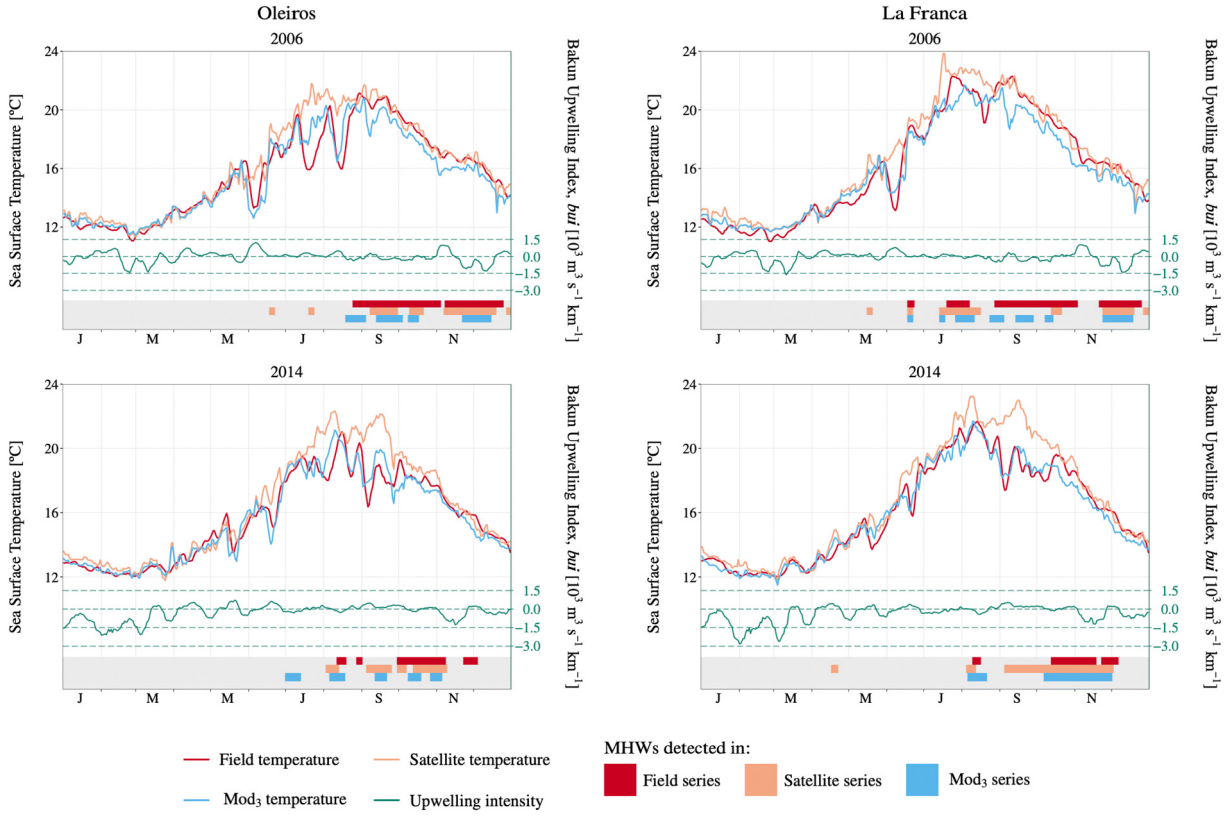


**Fig. 2.** Seasonal sea surface temperature variations at Oleiros (*left column*) and La Franca (*right column*) in 2006 (*top row*) and 2014 (*bottom row*). Colored bars in red (field), orange (satellite) and light blue (best selected model [$Mod_3$, Table 1]) show marine heatwave days detected with each temperature series. The years shown here are among those with the most remarkable marine heatwaves in number and/or intensity and/or duration in the entire series (1998–2019). The rest of the years are further illustrated in Fig. S3 & Fig. S4 in the Supplementary File.

Table S1). Warming rates increase eastwards towards the inner Bay of Biscay (Fig. S5 in Supplementary File).

The comparative analysis of MHW features based on static *vs.* dynamic detection thresholds pointed towards a potential role of long-term ocean warming in enhancing MHWs in the Cantabrian Sea in the past 40 years (Fig. 4). When using a static MHW detection threshold (left column in Fig. 4) both the number of MHW events and MHW days per year revealed an increase by a factor of ~1.9 per decade (*i.e.*, doubling each 11 years). No significant trends were found for $i_{max}$, $i_{mean}$, $i_{cum}$ and *dur* ($p$-value >0.05 in every computation), though all estimates were positive. When using a dynamic MHW detection threshold incorporating a linear warming trend in surface temperature (right column in Fig. 4), all trends became non-significant and estimates substantially decreased.

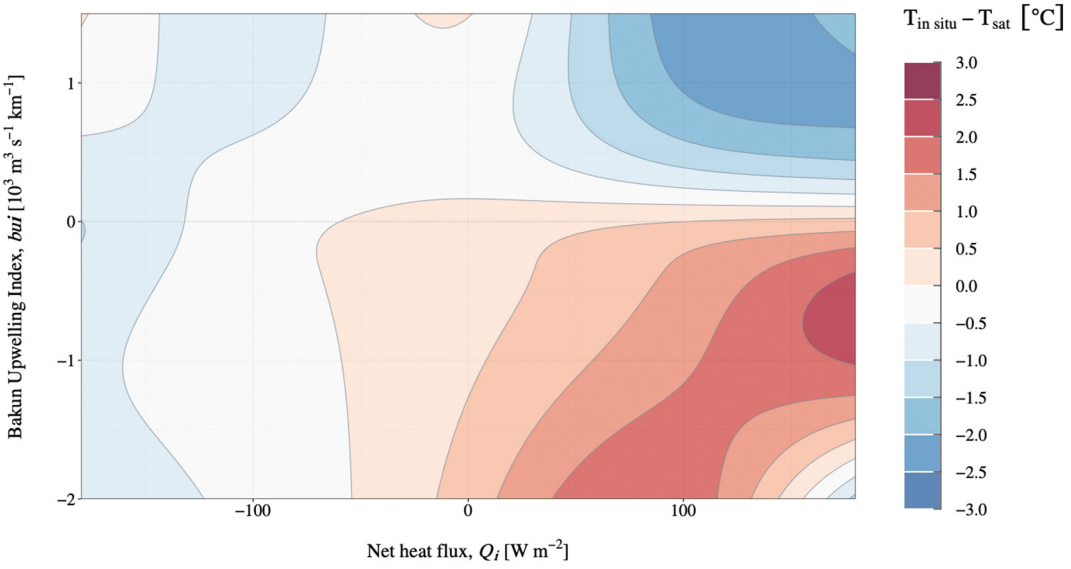


**Fig. 3.** Non-linear interaction between the Bakun Upwelling Index (*bui*) and net heat flux ($Q_i$) based on the best selected model ($Mod_3$, Table 1) on the difference between field and satellite temperatures.

**Table 3**
Assessment of detected MHW in satellite and model-based reconstructions of coastal temperatures with respect to those detected based on field observations. Presence-absence confusion matrices were built to compare the number of non-MHW and MHW days detected with the field measurements [reference] *vs.* those from the satellite and the best selected model -$Mod_3$, Table 1-, respectively [tests], within Jan. 1998 – Mar. 2019 at Oleiros and La Franca. For each approach, each date is classified as a *presence* (MHW) or as an *absence* (non-MHW) to calculate the numbers of: true positives (both test and reference are *presences*), false positives (*presence* in the test but *absence* in the reference), true negative (both test and reference are *absences*) and false negative (test is an *absence* but the reference is a *presence*).

| Confusion matrices | | | | | | | | | |
|---|---|---|---|---|---|---|---|---|---|
| | | Oleiros | | | | La Franca | | | |
| | | Satellite | | Model | | Satellite | | Model | |
| | | MHW | Non − MHW | MHW | Non − MHW | MHW | Non − MHW | MHW | Non − MHW |
| Field | MHW | 235 | 379 | 251 | 363 | 190 | 234 | 213 | 211 |
| | Non − MHW | 277 | 6364 | 202 | 6439 | 330 | 5775 | 210 | 5895 |

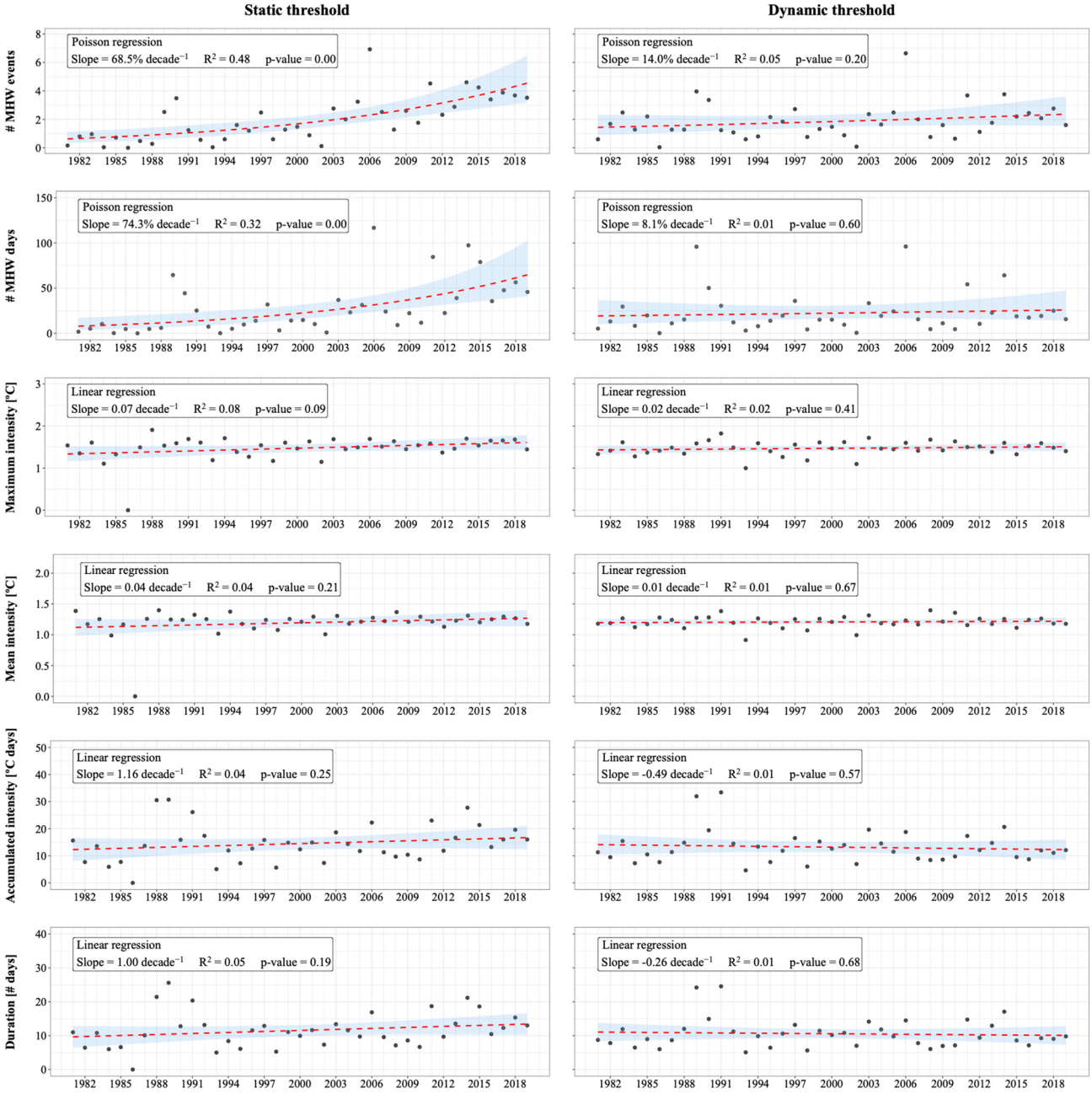


**Fig. 4.** Annual values -on average for all 25 localities along the Cantabrian coast- of the features of the marine heatwaves detected with the extended modelled series using a static (*left*) *vs.* a dynamic (*right*) baseline period. Red dashed lines indicate the estimate linear trend for each marine heatwave feature. The slope, proportion of variance explained ($R^2$), and *p*-value of each trend are shown. Shaded areas account for 95% confidence intervals.

To ease the interpretation of the increase in MHW incidence throughout the past 40 years, we arranged by decades the number of MHW days detected in the extended series (Fig. 5) and mapped them to illustrate spatial gradients along the Cantabrian coast (Fig. S6 in Supplementary File). On average for all 25 localities covering the spatial extent of the extended series, a total of 1047 *vs.* 839 MHW days per decade were detected in the past four decades when using static *vs.* dynamic detection thresholds, respectively (Fig. 5). This may be interpreted as 80% of MHW days (839/1047) taking place regardless of the underlying warming trend, while the remaining ~20% (208/1047) occurring because of it. The proportions increase to 60–40% for the period 2000–19, and to 50–50% for 2010–2019. The analysis also revealed considerable interannual and interdecadal variability, with some years having a remarkably high number of MHW days (*i.e.,* 2006, 2011 or 2014; Fig. 4). Overall, the analysis based on a static baseline period reveals a six-fold increase in the incidence of MHWs during the last four decades, which exceeds the two-fold, steady increase observed in the series derived using a dynamic threshold.

## 4. Discussion

This study combines two decades of field temperature measurements with long term reanalysis and satellite data in a statistical downscaling approach based on regression modeling, which allowed to reconstruct past coast-level temperatures and hindcast the incidence of MHW in the last four decades. By including the effect of coastal upwelling and air-sea heat fluxes, our method enabled us to predict an improved temperature series that i) reliably reproduces near-shore sea surface temperatures, ii) retains the satellite's spatial and temporal resolution and iii) improves MHW detection near-shore. Also, the assessment of trends using static *vs.* dynamic detection thresholds suggested that the underlying ocean warming trend contributed to enhance the incidence, intensity and duration of MHWs along the coasts of the Cantabrian Sea during the last four decades.

Downscaling of satellite data enabled the reconstruction of a temperature series to fairly capture temperature variation close to the coast, enhancing the detection and characterization of MHW nearshores. However, some aspects of this approach limit its possible application in other areas and require further refinement. The proposed downscaling approach relies on long-term field records of water temperature that are seldom available (Oliver et al., 2021). Data from meteorological station networks provide a potential alternative, with the added challenge of modeling water temperature dynamics (*e.g.*, Somavilla Cabrillo et al., 2011). Another caveat lies on the number of stations needed to properly characterize downscaling transfer functions. The two stations, Oleiros and La Franca, may not be fully representative of upwelling regimes along the southern Bay of Biscay, which tend to be weaker towards the inner part of the Bay (Lavín et al., 2006).

Our approach has room to improve by considering additional physical processes modulating water temperatures along the Cantabrian shelf, like the incidence of the Iberian Poleward Current (IPC, García-Soto et al., 2002). This current conveys subtropical, warm waters along the Cantabrian continental shelf and slope during winter, which result in milder conditions that might favor the occurrence of MHWs. In other areas, it may be more important to account for the impact of river discharge or tidal currents on temperature. Nevertheless, the approach provides reasonable, robust predictions and reassures the use of downscaling approaches to extend the applicability of coarse satellite and reanalysis products near the shore.

Disparities between field and satellite temperature records are compatible with those reported in prior studies regarding the reliability of nearshore satellite temperature data (Stobart et al., 2008; Smit et al., 2013; Stobart et al., 2016). The importance of these biases depends on the specific context and the question at hand. Analyses of short-term temperature extremes like MHWs, which entail fine-scale recording of swift temperature variations, may be compromised by small scale biases (Smale and Wernberg, 2009). On the other hand, satellites provide a reliable approach to assess the incidence and impact of surface MHWs in the open ocean (Fewings and Brown, 2019). Downscaling methods are routinely used to project climate variables from coarse-resolution climate models to a local-scale (*e.g.*, Gaitán et al., 2013; Gaitán, 2016; Muhling et al., 2017) and to reproduce historical records of specific events (Hirsch et al., 2021). Our approach relies on analyses of air-sea heat fluxes and estimates of wind-induced cross-shore transport to calibrate satellite estimates against field measurements through regression modeling.

Deviations between satellite and field temperature records during coastal upwelling events depend on water column stratification (Botas et al., 1990; Lavín et al., 2006; Llope et al., 2006), but they mainly reflect the coarse resolution of the satellite product employed here. First, temperature variability close to the land-sea margin occurs at smaller spatial scales than offshore and, as a result, the effect of local physical processes such as coastal upwelling might go unnoticed to it (Smit et al., 2013). Second, the coarse size of the satellite pixel entails an unavoidable interpolation with temperatures more offshore. In general, open ocean waters have a greater inertia and vary at a slower pace than shallow waters (Marin et al., 2021a). In particular, upwelling-prone coastal areas tend to present significant differences in warming rates when comparing trends in nearshore and offshore waters. Coastal cooling due to upwelling weakens trends in surface temperature (Gentemann et al., 2017; Fewings and Brown, 2019) and

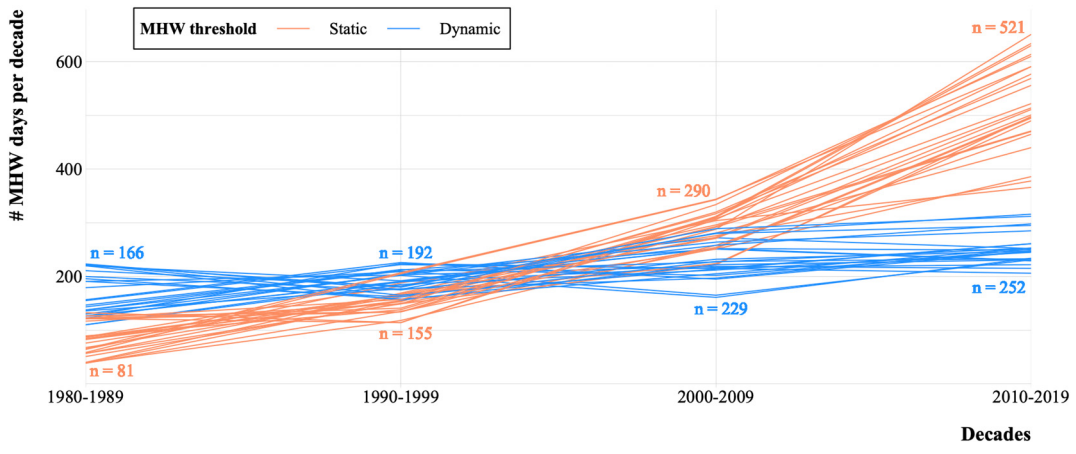


**Fig. 5.** Progression of the number of marine heatwave days decade$^{-1}$ detected with the extended modelled temperature series when calculated using static (blue) *vs.* dynamic (orange) detection thresholds (see left and middle columns in Fig. S6). Note that we adjusted the estimates by the total number of days per decade to compensate lack of data in the early 1980s. Each line -for each colour- represents one locality of the 25 examined along the Cantabrian coast. Numeric values indicate the average number of marine heatwaves per decade calculated using all 25 localities for each marine heatwave detection threshold approach.

enhances differences in warming rates between coastal and oceanic waters. Offshore waters remain unaffected by the cold-deep-water pump and experience higher warming rates (Santos et al., 2011; deCastro et al., 2014). In fact, Varela et al. (2018) found that SST warming has been more intense in offshore than nearshore waters in ~92% of the upwelling locations worldwide. During upwelling events, satellite retrievals of offshore temperatures may result in warmer measurements than those recorded by the field loggers close to the shore. Indeed, Meneghesso et al. (2020), revealed that Level 4 remotely-sensed products (blended satellite and/or *in situ* observations, interpolated to fill data gaps like those used here) can overestimate coastal SST in upwelling prone locations. This warm bias may consequently lead to the overestimation of MHW events. Varela et al. (2021) recently showed that trends in the number of MHW days were lower near the coast than in adjacent offshore areas in the Eastern Boundary Upwelling systems. Our results add to previous evidence showing a similar buffering effect in a system with weak seasonal upwelling and highlight how satellite-derived SSTs may overestimate MHW incidence near the coast.

All available estimates agree that the Bay of Biscay has been warming at rates above 0.1 °C per decade since the 1970s (Table S1). The increase in SST observed in the present study in all 25 localities along the coast of northern Spain within Sep. 1981–Dec. 2019 confirms previous findings and results in trend estimates similar to those of Gómez-Gesteira et al. (2008), who revealed a warming of 0.15–0.25 °C per decade along the Cantabrian coast. This temperature increase might be linked to the general warming trend in the North Atlantic Ocean, which is attributed to global climate change (Harris et al., 2014).

The combined use of static and dynamic detection thresholds allowed us to contrast MHW trends with and without the effect of long-term ocean warming (Oliver et al., 2021). The results imply that the underlying warming trend contributed to increase the number of MHW days in the Cantabrian coast by a 20% (Fig. 5 & Fig. S6). These outcomes are consistent with the assessment of the impact of global warming on MHW incidence conducted by Laufkötter et al. (2020) and Marin et al. (2021b).

The contrast in the trends obtained with each MHW detection threshold for all MHW features (Fig. 4) suggests that their overall increase has its origin in the progressive ocean warming trend. It should be noted that the warming period to which the Bay of Biscay is currently subjected began in the 1970s (deCastro et al., 2009). The extended modelled series comprises most of it; nonetheless, a time series spanning the warming period thoroughly may have likely revealed a clearer increasing trend for MHW features such as $i_{max}$ and $i_{mean}$ (Fig. 4). The observed differences in the progression of the number of MHW days per decade calculated with each detection threshold also pointed towards the effect of the underlying sea warming trend (Fig. 5 & Fig. S6). The static threshold series followed a quite accentuated trend from the very beginning though it reached maximum steepness from the 2000s on, coinciding with an increase in the SST warming rate in central Cantabrian Sea (Voerman et al., 2013).

Since the 1970s, the N coast of Spain has been subjected to a global warming-associated increase in SST (deCastro et al., 2009), especially during summer, enhancing water column stratification (González-Gil et al., 2015, 2018); this trend parallels a decrease in the number of upwelling days and their intensity, especially towards the inner part of the Bay of Biscay (Llope et al., 2006; Pérez et al., 2010; Gómez-Gesteira et al., 2011). Taken together, these trends may lead to an enhanced warming of the upper ocean layer in the coming years, which could be particularly remarkable during summer months (Llope et al., 2006). Coastal upwelling can abate SST anomalies in coastal areas (Gentemann et al., 2017; Fewings and Brown, 2019) and provide thermal refugia to cold-affinity species (Lourenço et al., 2016; Seabra et al., 2019). Our findings support the understanding of upwelling systems as key factors buffering ocean warming nearshore and preventing the impact of threatening climate extremes.

Cold-temperate canopy-forming macroalgae are key components of Cantabrian coastal marine ecosystems, as they provide complex habitat for a wide range of associated flora and fauna (Martínez et al., 2015). Several authors have recently reported the abundance decrease, retreat and redistribution of numerous macroalgae communities and their associated biodiversity since the end of the XX century (Fernández, 2011; Viejo et al., 2011; Duarte et al., 2013; Nicastro et al., 2013; Fernández, 2016; Casado-Amezúa et al., 2019; Ramos et al., 2020). These shifts have generally been attributed to the general increase in SST in the Cantabrian Sea; indeed, ocean warming has a negative effect on seaweed species (Wernberg et al., 2011b).

Long-term changes in mean SST are the main driver of the observed trends in the occurrence of coastal MHWs globally (Frölicher and Laufkötter, 2018; Oliver et al., 2019). Considering the above-described trends in the Cantabrian Sea, this hints at an alarming scenario for the coming years. Extreme temperature events tend to exert stronger, more immediate impacts than average gradual trends associated with ocean warming (Sanz-Lázaro, 2016; Oliver et al., 2018). In fact, MHWs have been accounted for remarkable impacts on macroalgae-dominated ecosystems around the world (Wernberg et al., 2011a; Wernberg et al., 2012; Smale and Wernberg, 2013; Reed et al., 2016; Wernberg and Straub, 2016; Wernberg et al., 2016; Arafeh-Dalmau et al., 2019). Extreme thermal stress derived from MHWs have well-documented effects on seaweeds (from resistance to altered physiological and ecological performance, disruption of ecosystem structure and regime shifts), although these may not be evident during, or immediately after SST peaks, but might rather have long time-lags (Straub et al., 2019). Overall, increasing temperatures and MHWs directly and indirectly alter the distribution and abundance of canopy-forming species. Thus, our findings highlight the high conservation value and the suitability of climate refugia associated with upwelling areas to safeguard seaweed diversity in the Cantabrian Sea.

The results in this study imply that, during the last decade, half of the MHW events detected along the Cantabrian coast occurred under the influence of the ocean warming trend. Future projections under different global warming scenarios predict an increase in the occurrence and intensity of MHWs in the coming years (Oliver et al., 2019). This urgently calls for a full risk assessment of the Cantabrian Sea marine organisms and ecosystems in order to encourage the elaboration of appropriate conservation and management strategies for a warmer future. The approach presented here might contribute to improve the monitoring of the impact of MHWs on marine coastal ecosystems, which remain key for human livelihood but are currently endangered under the threat of escalating global warming.

## CRediT authorship contribution statement

**Paula Izquierdo:** Conceptualization, Methodology, Formal analysis, Validation, Investigation, Writing – original draft, Writing – review & editing, Visualization. **Fernando González Taboada:** Conceptualization, Methodology, Formal analysis, Resources, Writing – review & editing, Visualization, Supervision. **Ricardo González-Gil:** Methodology, Formal analysis, Writing – review & editing, Visualization. **Julio Arrontes:** Investigation, Resources, Data curation, Writing – review & editing. **José M. Rico:** Conceptualization, Supervision, Resources.

## Declaration of competing interest

The authors declare that they have no known competing financial interests or personal relationships that could have appeared to influence the work reported in this paper.

## Acknowledgements

We thank the NOAA NESDIS and NCDC for the production, availability and maintenance of NOAA Optimum interpolation 0.25° daily sea surface temperature analysis.

We thank the reviewer for the time devoted to the improvement of this manuscript.

This is a contribution of the Asturian Marine Observatory (OMA) of the University of Oviedo. This research did not receive any specific grant from funding agencies in the public, commercial, or not-for-profit sectors. Temperature loggers are a part of the equipment financed by the OMA.

## Appendix A. Supplementary data

Supplementary data to this article can be found online at https://doi.org/10.1016/j.scitotenv.2022.155478.

## References


Allouche, O., Tsoar, A., Kadmon, R., 2006. Assessing the accuracy of species distribution models: prevalence kappa and the true skill statistic (TSS). J. Appl. Ecol. 43, 1223–1232. https://doi.org/10.1111/j.1365-2664.2006.01214.x.

Anadón, R., Niell, F.X., 1980. Distribución longitudinal de macrófitos en la costa asturiana (N de España). Investig. Pesq. 45 (1), 143–156.

Arafeh-Dalmau, N., Montaño-Moctezuma, G., Martínez, J.A., Beas-Luna, R., Schoeman, D.S., Torres-Moye, G., 2019. Extreme marine heatwaves alter kelp forest community near its equatorward distribution limit. Front. Mar. Sci. 6. https://doi.org/10.3389/fmars.2019.00499.

Bakun, A., 1973. Coastal Upwelling Indices, West Coast of North America, 1946-71. US Department of Commerce, National Oceanic and Atmospheric Administration, National Marine Fisheries Service SSRF-671, p. 103.

Banzon, V., Smith, T.M., Chin, T.M., Liu, C., Hankins, W., 2016. A long-term record of blended satellite and in situ sea-surface temperature for climate monitoring modeling and environmental studies. Earth Syst. Sci. Data 8, 165–176. https://doi.org/10.5194/essd-8-165-2016.

Barbier, E.B., 2017. Marine ecosystem services. Curr. Biol. 27, R507–R510. https://doi.org/10.1016/j.cub.2017.03.020.

Bolker, B., 2020. R Development Core Team. Bbmle: Tools for General Maximum Likelihood Estimation R package version 1.0.23.1.

Botas, J.A., Fernández, E., Bode, A., Anadón, R., 1990. A persistent upwelling off the Central Cantabrian Coast. Estuar. Coast. Shelf Sci. 30, 185–199.

Burnham, K.P., Anderson, D.R., 2002. Model Selection and Multimodel Inference: A Practical Information-Theoretic Approach. 2nd ed. Springer-Verlag.

Casado-Amezúa, P., Araújo, R., Bárbara, I., Bermejo, R., Borja, Á., Díez, I., et al., 2019. Distributional shifts of canopy-forming seaweeds from the Atlantic coast of Southern Europe. Biodivers. Conserv. 28, 1151–1172. https://doi.org/10.1007/s10531-019-01716-9.

Casey, K.S., Brandon, T.B., Cornillon, P., Evans, R., 2010. The past present, and future of the AVHRR Pathfinder SST Program. In: Barale, V., Gower, J.F.R., Alberotanza, L. (Eds.), Oceanography From Space: Revisited. Springer, pp. 273–287. https://doi.org/10.1007/978-90-481-8681-5_16.

Chandler, R.E., Scott, E.M., 2011. Statistical Methods for Trend Detection and Analysis in the Environmental Sciences. John Wiley & Sons https://doi.org/10.1002/9781119991571.

Chang, W., 2014. Extrafont: Tools for Using Fonts R package version 0.17.

Clarke, A., 2017. Principles of Thermal Ecology: Temperature, Energy and Life. Oxford University Press https://doi.org/10.1093/oso/9780199551668.001.0001.

Costanza, R., Groot, R., Sutton, P., van der Ploeg, S., Anderson, S.J., Kubiszewski, I., et al., 2014. Changes in the global value of ecosystem services. Glob. Environ. Chang. 26, 152–158. https://doi.org/10.1016/j.gloenvcha.2014.04.002.

deCastro, M., Gómez-Gesteira, M., Alvarez, I., Gesteira, J.L.G., 2009. Present warming within the context of cooling-warming cycles observed since 1854 in the Bay of Biscay. Cont. Shelf Res. 29, 1053–1059. https://doi.org/10.1016/j.csr.2008.11.016.

deCastro, M., Gómez-Gesteira, M., Costoya, X., Santos, F., 2014. Upwelling influence on the number of extreme hot SST days along the Canary upwelling ecosystem. J. Geophys. Res. Oceans 119, 3029–3040. https://doi.org/10.1002/2013JC009745.

Denny, M.W., Hunt, L.J.H., Miller, L.P., Harley, C.D.G., 2009. On the prediction of extreme ecological events. Ecol. Monogr. 79, 397–421. https://doi.org/10.1890/08-0579.1.

Dowle, M., Srinivasan, A., 2021. Data.table: Extension of 'data.frame' R package version 1.14.0.

Duarte, C.M., Agusti, S., Barbier, E., Britten, G.L., Castilla, J.C., Gattuso, J.P., et al., 2020. Rebuilding marine life. Nature 580, 39–51. https://doi.org/10.1038/s41586-020-2146-7.

Duarte, L., Viejo, R.M., Martínez, B., deCastro, M., Gómez-Gesteira, M., Gallardo, T., 2013. Recent and historical range shifts of two canopy-forming seaweeds in North Spain and the link with trends in sea surface temperature. Acta Oecol. 51, 1–10. https://doi.org/10.1016/j.actao.2013.05.002.

Fernández, C., 2011. The retreat of large brown seaweeds on the north coast of Spain: the case of Saccorhiza polyschides. Eur. J. Phycol. 46, 352–360. https://doi.org/10.1080/09670262.2011.617840.

Fernández, C., 2016. Current status and multidecadal biogeographical changes in rocky intertidal algal assemblages: the northern Spanish coast. Estuar. Coast. Shelf Sci. 171, 35–40. https://doi.org/10.1016/j.ecss.2016.01.026.

Fewings, M.R., Brown, K.S., 2019. Regional structure in the marine heat wave of summer 2015 off the Western United States. Front. Mar. Sci. 6. https://doi.org/10.3389/fmars.2019.00564.

Fox-Kemper, B., Hewitt, H.T., Xiao, C., Aðalgeirsdóttir, G., Drijfhout, S.S., Edwards, T.L., et al., 2021. Ocean, cryosphere and sea level change. Climate Change 2021: The Physical Science Basis. Contribution of Working Group I to the Sixth Assessment Report of the Intergovernmental Panel on Climate Change. Cambridge University Press.

Frölicher, T.L., Laufkötter, C., 2018. Emerging risks from marine heat waves. Nat. Commun. 9, 650. https://doi.org/10.1038/s41467-018-03163-6.

Frölicher, T.L., Fischer, E.M., Gruber, N., 2018. Marine heatwaves under global warming. Nature 560, 360–364. https://doi.org/10.1038/s41586-018-0383-9.

Gaitán, C., 2016. Effects of variance adjustment techniques and time-invariant transfer functions on heat wave duration indices and other metrics derived from downscaled time-series. Study case: Montreal, Canada. Nat. Hazards. https://doi.org/10.1007/s11069-016-2381-2.

Gaitán, C., Hsieh, W., Cannon, A., Gachon, P., 2013. Evaluation of linear and non-linear downscaling methods in terms of daily variability and climate indices: surface temperature in southern Ontario and Quebec, Canada. Atmosphere-Ocean 52 (3), 211–221. https://doi.org/10.1080/07055900.2013.857639.

García-Reyes, M., Largier, J., 2010. Observations of increased wind-driven coastal upwelling off central California. J. Geophys. Res. 115, C04011. https://doi.org/10.1029/2009JC005576.

García-Soto, C., Pingree, R.D., Valdés, L., 2002. Navidad development in the southern Bay of Biscay: climate change and swoddy structure from remote sensing and in situ measurements. J. Geophys. Res. 107 (C8). https://doi.org/10.1029/2001jc001012.

GEBCO Compilation Group, 2021. GEBCO 2021 Grid.

Gelman, A., Hill, J., 2007. Data Analysis Using Regression and Multilevel/Hierarchical Models. Cambridge University Press https://doi.org/10.1017/CBO9780511790942.

Gentemann, L., Fewings, M.R., García-Reyes, M., 2017. Satellite Sea surface temperatures along the West Coast of the United States during the 2014–2016 northeast Pacific marine heat wave. Geophys. Res. Lett. 44, 312–319. https://doi.org/10.1002/2016GL071039.

Gil, J., Valdés, L., Moral, M., Sánchez, R., García-Soto, C., 2002. Mesoscale variability in a high-resolution grid in the Cantabrian Sea (southern Bay of Biscay) may 1995. Deep-Sea Res. I Oceanogr. Res. Pap. 49, 1591–1607. https://doi.org/10.1016/S0967-0637(02)00041-9.

GMAO Global Modeling & Assimilation Office, n.d.GMAO Global Modeling & Assimilation Office. MERRA-2 tavg1_2d_ocn_Nx: 2d, 1-Hourly, Time-Averaged, Single-Level, Assimilation, Ocean Surface Diagnostics V5.12.4. Greenbelt, MD, USA, Goddard Earth Sciences Data and Information Services Center (GES DISC) Accessed: [Mon, November 30, 2020].

Gómez-Gesteira, M., deCastro, M., Alvarez, I., Gómez-Gesteira, J., 2008. Coastal sea surface temperature warming trend along the continental part of the Atlantic Arc (1985–2005). J. Geophys. Res. 113 (C4). https://doi.org/10.1029/2007jc004315.

Gómez-Gesteira, M., Gimeno, L., deCastro, M., Lorenzo, M.N., Alvarez, I., Nieto, R., et al., 2011. The state of climate in NW Iberia. Clim. Res. 48, 109–144. https://doi.org/10.3354/cr00967.

González-Gil, R., Taboada, F., Höfer, J., Anadón, R., 2015. Winter mixing and coastal upwelling drive long-term changes in zooplankton in the Bay of Biscay (1993–2010). J. Plankton Res. 37 (2), 337–351. https://doi.org/10.1093/plankt/fbv001.

González-Gil, R., González Taboada, F., Cáceres, C., Largier, J., Anadón, R., 2018. Winter-mixing preconditioning of the spring phytoplankton bloom in the Bay of Biscay. Limnol. Oceanogr. 63 (3), 1264–1282. https://doi.org/10.1002/lno.10769.

Grolemund, G., Wickham, H., 2011. Dates and times made easy with lubridate. J. Stat. Softw. 40 (3), 1–25. https://doi.org/10.18637/jss.v040.i03.

Gulev, S.K., Thorne, P.W., Ahn, J., Dentener, F.J., Domingues, C.M., Gerland, S., et al., 2021. Changing state of the climate system. Climate Change 2021: The Physical Science Basis. Contribution of Working Group I to the Sixth Assessment Report of the Intergovernmental Panel on Climate Change. Cambridge University Press In Press.

Harris, V., Edwards, M., Olhede, S.C., 2014. Multidecadal Atlantic climate variability and its impact on marine pelagic communities. J. Mar. Syst. 133, 55–69. https://doi.org/10.1016/j.jmarsys.2013.07.001.

Hastie, T., Tibshirani, R., 1986. Generalized additive models. Stat. Sci. 43, 297–310. https://doi.org/10.1214/ss/1177013604.

Hersbach, H., Bell, B., Berrisford, P., Biavati, G., Horányi, A., Sabater, J.M., et al., 2020. ERA5 hourly data on single levels from 1979 to present. Q. J. R. Meteorol. Soc. 146, 1999–2049. https://doi.org/10.1002/qj.3803.

Hirsch, A., Ridder, N., Perkins-Kirkpatrick, S., Ukkola, A., 2021. CMIP6 MultiModel evaluation of present-day heatwave attributes. Geophys. Res. Lett. 48 (22). https://doi.org/10.1029/2021gl095161.

Hobday, A.J., Alexander, L.V., Perkins, S.E., Smale, D.A., Straub, S.C., Oliver, E.C.J., et al., 2016. A hierarchical approach to defining marine heatwaves. Prog. Oceanogr. 141, 227–238. https://doi.org/10.1016/j.pocean.2015.12.014.

Koutsikopoulos, C., Beillois, P., Leroy, C., Taillefer, F., 1998. Temporal trends and spatial structures of the sea surface temperature in the Bay of Biscay. Oceanol. Acta 21, 335–344. https://doi.org/10.1016/S0399-1784(98)80020-0.

Kuhn, M., 2020. Caret: Classification and Regression Training R package version 6.0-86.

Large, W.G., McWilliams, J.C., Doney, S.C., 1994. Oceanic vertical mixing: a review and a model with a nonlocal boundary layer parameterization. Rev. Geophys. 32, 363–403. https://doi.org/10.1029/94RG01872.

Laufkötter, C., Zscheischler, J., Frölicher, T.L., 2020. High-impact marine heatwaves attributable to human-induced global warming. Science 369, 1621–1625. https://doi.org/10.1126/science.aba0690.

Lavín, A., Valdés, L., Sánchez, F., Abaunza, P., Forest, A., et al., Boucher, 2006. The Bay of Biscay: the encountering of the ocean and the shelf (18b, E). The Sea. 14, pp. 933–999.

Llope, M., Anadón, R., Viesca, L., Quevedo, M., González-Quirós, R., et al., Stenseth, 2006. Hydrography of the southern Bay of Biscay shelf-break region: integrating the multiscale physical variability over the period 1993-2003. J. Geophys. Res. 111. https://doi.org/10.1029/2005JC002963.

Lourenço, C., Zardi, G., McQuaid, C., Serrão, E., Pearson, G., Jacinto, R., Nicastro, K., 2016. Upwelling areas as climate change refugia for the distribution and genetic diversity of a marine macroalga. J. Biogeogr. 43 (8), 1595–1607. https://doi.org/10.1111/jbi.12744.

Macreadie, P., Costa, M., Atwood, T., Friess, D., Kelleway, J., Kennedy, H., et al., 2021. Blue carbon as a natural climate solution. Nat. Rev. Earth Environ. https://doi.org/10.1038/s43017-021-00224-1.

Marin, M., Bindoff, N., Feng, M., Phillips, H., 2021a. Slower long-term coastal warming drives dampened trends in coastal marine heatwave exposure. J. Geophys. Res. Oceans 126 (11). https://doi.org/10.1029/2021jc017930.

Marin, M., Feng, M., Phillips, H.E., Bindoff, N.L., 2021b. A global multiproduct analysis of coastal marine heatwaves: distribution, characteristics, and long-term trends. J. Geophys. Res. Oceans 126. https://doi.org/10.1029/2020JC016708.

Martínez, B., Afonso-Carrillo, J., Anadón, R., Araújo, R., Arenas, F., Arrontes, J., et al., 2015. Regresión de las algas marinas en la costa Atlántica de la Península Ibérica y en las Islas Canarias por efecto del cambio climático. 49. ALGAS, Boletín Informativo de la Sociedad Española de Ficología.

Meneghesso, C., Seabra, R., Broitman, B., Wethey, D., Burrows, M., Chan, B., et al., 2020. Remotely-sensed L4 SST underestimates the thermal fingerprint of coastal upwelling. Remote Sens. Environ. 237, 111588. https://doi.org/10.1016/j.rse.2019.111588.

Muhling, B., Gaitán, C., Stock, C., Saba, V., Tommasi, D., Dixon, K., 2017. Potential salinity and temperature futures for the Chesapeake Bay using a statistical downscaling spatial disaggregation framework. Estuar. Coasts 41 (2), 349–372. https://doi.org/10.1007/s12237-017-0280-8.

Neuwirth, E., 2014. RcolorBrewer: ColorBrewer Palettes R package version 1.1-2.

Nicastro, K.R., Zardi, G.I., Teixeira, S., Neiva, J., Serrão, E.A., Pearson, G.A., 2013. Shift happens: trailing edge contraction associated with recent warming trends threatens a distinct genetic lineage in the marine macroalga Fucus vesiculosus. BMC Biol. 11. https://doi.org/10.1186/1741-7007-11-6.

Nychka, D., Furrer, R., Paige, J., Sain, S., 2017. fields: Tools for Spatial Data R package version 11.6.

O'Leary, J.K., Micheli, F., Airoldi, L., Boch, C., De Leo, G., Elahi, R., et al., 2017. The resilience of marine ecosystems to climatic disturbances. Bioscience 67, 208–220. https://doi.org/10.1093/biosci/biw161.

Oliver, E., Burrows, M., Donat, M., Sen Gupta, A., Alexander, L., Perkins-Kirkpatrick, S., et al., 2019. Projected marine heatwaves in the 21st century and the potential for ecological impact. Front. Mar. Sci. 6. https://doi.org/10.3389/fmars.2019.00734.

Oliver, E.C.J., Donat, M.G., Burrows, M.T., Moore, P.J., Smale, D.A., Alexander, L.V., et al., 2018. Longer and more frequent marine heatwaves over the past century. Nat. Commun. 9 (1), 1324. https://doi.org/10.1038/s41467-018-03732-9.

Oliver, E.C.J., Benthuysen, J.A., Darmaraki, S., Donat, M.G., Hobday, A.J., Holbrook, N.J., et al., 2021. Marine heatwaves. Annu. Rev. Mar. Sci. 13, 313–342. https://doi.org/10.1038/ncomms16101.

Otero, P., Ruiz-Villarreal, M., 2008. Wind forcing of the coastal circulation off north and northwest Iberia: comparison of atmospheric models. J. Geophys. Res. 113, C10019. https://doi.org/10.1029/2008JC004740.

Pebesma, E., 2018. Simple features for R: standardized support for spatial vector data. R J. 10 (1), 439–446. https://doi.org/10.32614/RJ-2018-009.

Pérez, F.F., Padín, X.A., Pazos, Y., Gilcoto, M., Cabanas, J.M., et al., Pardo, 2010. Plankton response to weakening of the Iberian coastal upwelling. Glob. Chang. Biol. 16, 1258–1267. https://doi.org/10.1111/j.1365-2486.2009.02125.x R package version 0.17.

Pierce, D., 2019. Ncdf4: Interface to Unidata netCDF (Version 4 or Earlier) Format Data Files R package version 1.17.

R Core Team, 2021. R: a language and environment for statistical computing. R Foundation for Statistical Computing, Vienna, Austria. https://www.R-project.org/.

Ramos, E., Guinda, X., Puente, A., de la Hoz, C.F., Juanes, J.A., 2020. Changes in the distribution of intertidal macroalgae along a longitudinal gradient in the northern coast of Spain. Mar. Environ. Res. 157, 104930. https://doi.org/10.1016/j.marenvres.2020.104930.

Reed, D., Washburn, L., Rassweiler, A., Miller, R., Bell, T., Harrer, S., 2016. Extreme warming challenges sentinel status of kelp forests as indicators of climate change. Nat. Commun. 7. https://doi.org/10.1038/ncomms13757.

Reynolds, R.W., Chelton, D.B., 2010. Comparisons of daily sea surface temperature analyses for 200708. J. Clim. 23, 3545–3562. https://doi.org/10.1175/2010JCLI3294.1.

Reynolds, R.W., Smith, T.M., Liu, C., Chelton, D.B., Casey, K.S., Schlax, M.G., 2007. Daily high-resolution-blended analyses for sea surface temperature. J. Clim. 20, 5473–5496. https://doi.org/10.1175/2007JCLI1824.1 American Meteorological Society, 2007.

Rhein, M., Rintoul, S.R., Aoki, S., Campos, E., Chambers, D., Feely, R.A., et al., 2013. Climate change 2013. Chapter 3. The Physical Science Basis. Contribution of Working Group I to the Fifth Assessment Report of the Intergovernmental Panel on Climate Change. Observations: Ocean. Cambridge University Press, Cambridge, United Kingdom and New York, NY, USA.

Santos, F., Gómez Gesteira, M., deCastro, M., 2011. Coastal and oceanic SST variability along the western Iberian Peninsula. Cont. Shelf Res. 31 (19–20), 2012–2017. https://doi.org/10.1016/j.csr.2011.10.005.

Sanz-Lázaro, C., 2016. Climate extremes can drive biological assemblages to early successional stages compared to several mild disturbances. Sci. Rep. 6. https://doi.org/10.1038/srep30607.

Schlegel, R.W., 2017. Coastal Marine Heatwaves: Understanding Extreme Forces. University of the Western Cape, Department of Biodiversity & Conservation Biology PhD Thesis.

Schlegel, R.W., Smit, A.J., 2018. heatwaveR: a central algorithm for the detection of heatwaves and cold-spells. J. Open Source Softw. 3 (27), 821. https://doi.org/10.21105/joss.00821.

Schlegel, R.W., Oliver, E.C.J., Hobday, A.J., Smit, A.J., 2019. Detecting marine heatwaves with sub-optimal data. Front. Mar. Sci. 6. https://doi.org/10.3389/fmars.2019.00737.

Seabra, R., Varela, R., Santos, A., Gómez-Gesteira, M., Meneghesso, C., Wethey, D., Lima, F., 2019. Reduced nearshore warming associated with eastern boundary upwelling systems. Front. Mar. Sci. 6. https://doi.org/10.3389/fmars.2019.00104.

Simpson, G.L., 2021. Gratia: Graceful 'ggplot'-Based Graphics and Other Functions for GAMs Fitted Using 'mgcv' R package version 0.5.1.

Simpson, J.H., Sharples, J., 2012. Introduction to the Physical and Biological Oceanography of Shelf Seas. Cambridge University Press.

Smale, D.A., Wernberg, T., 2009. Satellite-derived SST data as a proxy for water temperature in nearshore benthic ecology. Mar. Ecol. Prog. Ser. 387, 27–37. https://doi.org/10.3354/meps08132.

Smale, D.A., Wernberg, T., 2013. Extreme climatic event drives range contraction of a habitat-forming species. Proc. R. Soc. B 280, 20122829.

Smit, A.J., Roberts, M., Anderson, R.J., Dufois, F., Dudley, S.F.J., Bornman, T.G., et al., 2013. A coastal seawater temperature dataset for biogeographical studies: large biases between in situ and remotely-sensed data sets around the coast of South Africa. PloS ONE 8, e81944. https://doi.org/10.1371/journal.pone.0081944.

Somavilla Cabrillo, R., González-Pola, C., Ruiz-Villarreal, M., Lavín Montero, A., 2011. Mixed layer depth (MLD) variability in the southern Bay of Biscay. Deepening of winter MLDs concurrent with generalized upper water warming trends? Ocean Dyn. 61 (9), 1215–1235. https://doi.org/10.1007/s10236-011-0407-6.

South, A., 2017. rnaturalearth: World Map Data from Natural Earth R package version 0.1.0.

Stobart, B., Downing, N., Buckley, R., Teleki, K., 2008. Comparison of in situ temperature data from the southern Seychelles with SST data: can satellite data alone be used to predict coral bleaching events? 'Proceedings of the 11th International Coral Reef Symposium', 7–11 July 2008, Fort Lauderdale, FL, USA, pp. 652–656

Stobart, B., Mayfield, S., Mundy, C., Hobday, A.J., Hartog, J.R., 2016. Comparison of in situ and satellite sea surface-temperature data from South Australia and Tasmania: how reliable are satellite data as a proxy for coastal temperatures in temperate southern Australia? Mar. Freshw. Res. 67, 612. https://doi.org/10.1071/MF14340.

Straub, S., Wernberg, T., Thomsen, M., Moore, P., Burrows, M., Harvey, B., Smale, D., 2019. Resistance, extinction, and everything in between – the diverse responses of seaweeds to marine heatwaves. Front. Mar. Sci. 6. https://doi.org/10.3389/fmars.2019.00763.

Varela, R., Lima, F., Seabra, R., Meneghesso, C., Gómez-Gesteira, M., 2018. Coastal warming and wind-driven upwelling: a global analysis. Sci. Total Environ. 639, 1501–1511. https://doi.org/10.1016/j.scitotenv.2018.05.273.

Varela, R., Rodríguez-Díaz, L., de Castro, M., Gómez-Gesteira, M., 2021. Influence of eastern upwelling systems on marine heatwaves occurrence. Glob. Planet. Chang. 196, 103379. https://doi.org/10.1016/j.gloplacha.2020.103379.

Viejo, R.M., Martínez, B., Arrontes, J., Astudillo, C., Hernández, L., 2011. Reproductive patterns in central and marginal populations of a large brown seaweed: drastic changes at the southern range limit. Ecography 34, 75–84. https://doi.org/10.1111/j.1600-0587.2010.06365.x.

Voerman, S.E., Llera, E., Rico, J.M., 2013. Climate driven changes in subtidal kelp forest communities in NW Spain. Mar. Environ. Res. 90, 119–127. https://doi.org/10.1016/j.marenvres.2013.06.006.

Wernberg, T., Straub, S.C., 2016. Impacts and effects of ocean warming on seaweeds. In: Laffoley, D., Baxter, J.M. (Eds.), 2016. Explaining Ocean Warming: Causes, Scale, Effects and Consequences. Full Report. IUCN, Gland, Switzerland, pp. 87–103.

Wernberg, T., Russell, B.D., Moore, P.J., Ling, S.D., Smale, D.A., Campbell, A., et al., 2011a. Impacts of climate change in a global hotspot for temperate marine biodiversity and ocean warming. J. Exp. Mar. Biol. Ecol. 400, 7–16. https://doi.org/10.1016/j.jembe.2011.02.021.

Wernberg, T., Russell, B., Thomsen, M., Gurgel, C., Bradshaw, C., Poloczanska, E., Connell, S., 2011b. Seaweed communities in retreat from ocean warming. Curr. Biol. 21 (21), 1828–1832. https://doi.org/10.1016/j.cub.2011.09.028.

Wernberg, T., Smale, D.A., Tuya, F., Thomsen, M.S., Langlois, T.J., de Bettignies, T., et al., 2012. An extreme climatic event alters marine ecosystem structure in a global biodiversity hotspot. Nat. Clim. Chang. 3, 78–82. https://doi.org/10.1038/nclimate1627.

Wernberg, T., Bennett, S., Babcock, R.C., de Bettignies, T., Cure, K., et al., Depczynski, 2016. Climate-driven regime shift of a temperate marine ecosystem. Science 353, 169–172. https://doi.org/10.1126/science.aad8745.

Wickham, H., 2007. Reshaping data with the reshape package. J. Stat. Softw. 21 (12), 1–20. https://doi.org/10.18637/jss.v021.i12.

Wickham, H., 2011. The split-apply-combine strategy for data analysis. J. Stat. Softw. 40 (1), 1–29. https://doi.org/10.18637/JSS.V040.I01.

Wickham, H., Averick, M., Bryan, J., Chang, W., McGowan, L., François, R., et al., 2019. Welcome to the Tidyverse. J. Open Source Softw. 4, 1686. https://doi.org/10.21105/joss.01686.

Wilby, R., Wigley, T., 1997. Downscaling general circulation model output: a review of methods and limitations. Prog. Phys. Geogr.: Earth Environ. 21 (4), 530–548. https://doi.org/10.1177/030913339702100403.

Wilke, C.O., 2020. Cowplot: Streamlined Plot Theme and Plot Annotations for 'ggplot2' R package version 1.1.1.

WMO, 2018. Guide to Climatological Practices. World Meteorological Organization, Geneva.

Wood, S.N., 2017. Generalized Additive Models: An Introduction With R. Chapman and Hall/CRC https://doi.org/10.1201/9781315370279.

Zeileis, A., Grothendieck, G., 2005. Zoo: S3Infrastructure for regular and irregular time series. J. Stat. Softw. 14. https://doi.org/10.18637/jss.v014.i06.